Evolution of magnetic domain structure of martensite in Ni–Mn–Ga films under the interplay of the temperature and magnetic field*

Xie Ren(谢 忍)[a], Wei Jun(韦 俊)[a], Liu Zhong-Wu(刘仲武)[b], Tang Yan-Mei(唐妍梅)[a], Tang Tao(唐 涛)[a], Tang Shao-Long(唐少龙)[a]†, and Du You-Wei(都有为)[a]

[a] *National Laboratory of Microstructures, Jiangsu Provincial Laboratory for Nanotechnology and Department of Physics, Nanjing University, Nanjing* 210093, *China*

[b] *School of Materials Science and Engineering, South China University of Technology, Guangzhou* 510640, *China*

(Received 18 October 2013; revised manuscript received 18 February 2013; published online 20 April 2014)

Ferromagnetic shape memory Ni–Mn–Ga films with 7M modulated structure were prepared on MgO (001) substrates by magnetron sputtering. Magnetization process with a typical two-hysteresis loop indicates the occurrence of the reversible magnetic field-induced reorientation. Magnetic domain structure and twin structure of the film were controlled by the interplay of the magnetic and temperature field. With cooling under an out-of-plane magnetic field, the evolution of magnetic domain structure reveals that martensitic transformation could be divided into two periods: nucleation and growth. With an in-plane magnetic field applied to a thermomagnetic-treated film, the evolution of magnetic domain structure gives evidence of a reorientation of twin variants of martensite. A microstructural model is described to define the twin structure and to produce the magnetic domain structure at the beginning of martensitic transformation; based on this model, the relationship between the twin structure and the magnetic domain structure for the treated film under an in-plane field is also described.

Keywords: Ni–Mn–Ga film, martensitic transformation, magnetically induced reorientation, magnetic domain structure

PACS: 81.40.–z, 75.70.Kw, 75.70.–i, 75.80.+q **DOI:** 10.1088/1674-1056/23/6/068103

1. Introduction

Ni–Mn–Ga is a ferromagnetic shape memory alloy (FSMA), attracting increasing interest due to its large magnetic-field-induced strain (MFIS). It is well known that the existence and efficiency of MFIS is determined by the magnetic-field-induced reorientation (MIR) of martensitic variants.[1–3] For the MIR effect, a magnetic field is employed to modify the martensitic structure by increasing the fraction of those martensitic variants that have easy magnetization axes parallel to the external field. The noncubic lattice of the martensite is reoriented by about 90° via twin boundary motion driven by the magnetic field, leading to a large change of dimension, namely MFIS.[4,5] The maximum strain is given by the difference in the lattice constants, and macroscopic strain up to 12% has been achieved in the Ni–Mn–Ga alloy.[3] The MIR effect is of interest for potential applications of FSMAs in magnetic actuators, sensors, and magnetoresistance.[6–8]

For applications in microdevices, the active materials have to be prepared in the form of films. At present, the investigations of the Ni–Mn–Ga films have mostly focused on the realization and proof of the MIR effect.[9–12] A majority of the results in the literature reveal that films affixed to a rigid substrate show no discernible MIR effect, even though they exhibit a well-defined martensitic transformation. Recent progress, however, has shown that the films exhibit a partial MIR effect.[9,10] It was also found that, in contrast to single-crystal bulk materials, the films show a reversible MIR effect even in the absence of external stresses.[11] This unusual response has been attributed to the fact that the films are grown on substrates. Naturally, the film must reorient in a manner which preserves its overall in-plane dimensions. Recognizing this constraint, a mode was proposed[9,10] by which the reorientation could take place for orthorhombic films with a grain structure containing {100}-oriented grains. In their mode the martensite variant reorientation was promoted by increasing the fraction of unit cells with the b axis parallel to the field at the expense of the unit cells with the a axis and c axis in the field direction. The self-reversibility of MIR was facilitated by substrate-imposed stresses which resisted the reorientation process.[9] Zhang *et al.*[11] described an alternative mode for the [101]-orientated films with crystal structure of $a = b > c$, they also suggested that the self-reversible MIR is determined by the interplay of MIR-active and MIR-inactive twin variants; the MIR-active variants are responsible for the de-twinning, while the latter imposes a restoring force on the MIR-active variants when they reorient.

MIR occurs in the low temperature martensitic phase. Of course, a description of the twinning structure of martensite is a prerequisite for a discussion of MIR. Meanwhile, the mag-

*Project supported by the National Key Project of Fundamental Research of China (Grant No. 2012CB932304), the National Natural Science Foundation of China (Grant No. 50831006), and the Program for New Century Excellent Talents in University (Grant No. NCET-11-0156), and the Priority Academic Program Development of Jiangsu Higher Education Institutions.

†Corresponding author. E-mail: tangsl@nju.edu.cn

© 2014 Chinese Physical Society and IOP Publishing Ltd

netic, mechanical, and magnetomechanical properties of Ni–Mn–Ga alloys depend strongly on the martensite structure and twin structure. The twin microstructure can be varied through suitable thermomagnetic tuning. In this paper, we provide an approach to control the magnetic domain structure as well as twin structure for {101}-oriented films with crystal structure of $a > b > c$ by the interplay of the magnetic field and the temperature field; based on the relationship of microstructure and the magnetic domain structure, the modified magnetic domain structure gives evidence of the reorientation of twin variants of the martensite.

2. Experiments

Ni–Mn–Ga films were deposited on MgO (001) substrates in argon atmosphere of 0.3 Pa at various temperatures from 673 K to 923 K by means of DC magnetron sputtering. The film deposited at 873 K was selected for further investigation. The sputtering 2″ target, with a nominal composition of $Ni_{52}Mn_{24}Ga_{24}$, was a wire-electrode cut from an ingot that had been induction-melted with high-purity elements three times to become homogeneous. A base pressure of better than 2×10^{-5} Pa was achieved to avoid the oxidation of the films, high purity argon atmosphere was introduced during sputtering; the substrate-to-target distance was 6.5 cm; and the sputtering power was maintained at 100 W, resulting in a growth rate of 0.74 nm/s. The 900-nm thickness of the films was controlled by sputtering time and confirmed by step profiler.

Energy dispersive X-ray analysis revealed a film composition of $Ni_{52.8}Mn_{23.4}Ga_{23.8}$ with an accuracy of 0.5 at.%. The crystallographic structure of the films was analyzed by X-ray diffraction (XRD, Panalytical X.Pert PRO type) with Cu-K_α radiation. Magnetic properties, including $M(H)$ and $M(T)$ curves, were measured using vibration sample magnetometer (Lakeshore). The atomic force microscopy (AFM) and magnetic force microscopy (MFM) observations were performed with a commercial scanning probe microscope (SPM, Veeco diDimension V) equipped with an in-house-built magnet fixture, allowing us to apply an alterable magnetic field up to 0.35 T parallel to the film-plane. A permanent magnet was attached to the bottom of the specimen to provide a fixed field of 0.02 T or 0.12 T, normal to the film plane. Topographic (height contrast) and magnetic (phase contrast) images were obtained in tapping and tapping-lift mode, respectively. All the AFM and MFM images were obtained with a scan rate of 0.3 Hz and scan range of 20×20 μm.

3. Results and discussion

The transformation temperatures M_s, M_f, A_s, and A_f, defining the start and finish temperatures for the forward and reverse martensitic transformations, were determined by measuring the temperature dependence of the magnetization under the magnetic field of 0.01 T, parallel to the film-plane (Fig. 1(a)). Because the magnetocrystalline anisotropy of martensite is higher than that of austenite, the film in martensitic state shows lower magnetization under low magnetic field of 0.01 T,[13] resulting in a thermal hysteresis centered at 310 K. This rectangular hysteresis clearly gives $M_s = 309$ K, $M_f = 305$ K, $A_s = 313$ K, and $A_f = 317$ K. It is also concluded that no other intermartensitic transformation takes place between 200 K and 400 K. The X-ray spectrum is displayed in the inset of Fig. 1(a). The three overlapping peaks can be indexed as an orthorhombic structure with the lattice constants: $a = 0.610$ nm, $b = 0.581$ nm, and $c = 0.555$ nm, indicating the 7M modulated martensitic phase. The martensitic {202} peak dominates the polycrystalline diffraction pattern, suggesting a strong degree of texture, i.e., the film contains [101]-oriented grains. This 7M martensitic structure has the possibility of realizing MIR.[4]

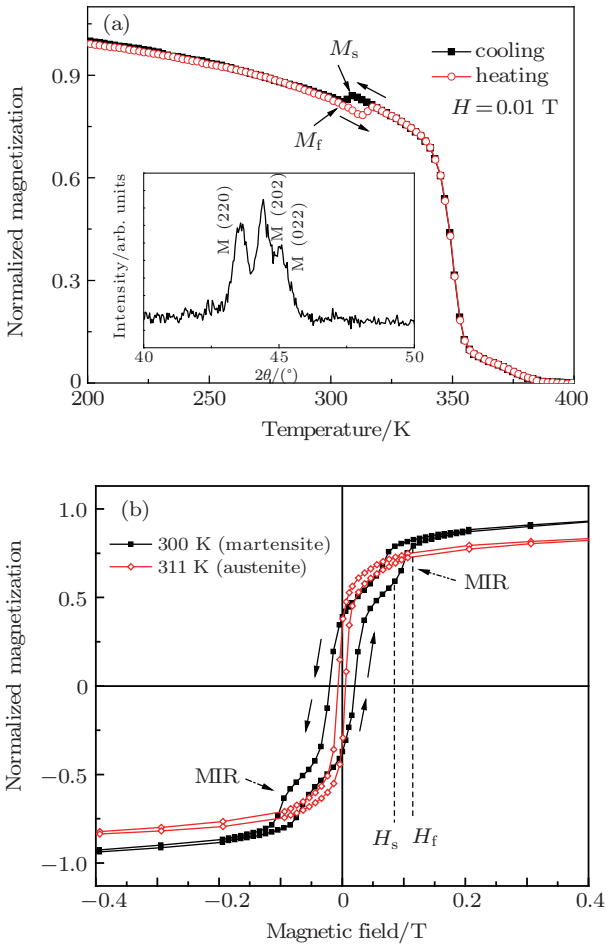


Fig. 1. (color online) (a) Normalized magnetization as a function of temperature, measured in a field of 0.01 T parallel to the film-plane, during cooling and heating (marked by arrows). Inset: X-ray diffraction, recorded at room temperature, of the film deposited on MgO (001). (b) Magnetization as a function of magnetic field during cooling, measured in the film plane at 300 K (martensite, black line) and 311 K (austenite, red line).

Magnetic hysteresis loops measured at 311 K and 300 K during cooling are shown in Fig. 1(b). The loops were measured in the film plane to avoid the influence of the demagnetization field. The hysteresis of the film in the austenitic state (at 311 K seen in Fig. 1(b)) provides a common single phase loop with a low coercivity due to low magnetocrystalline anisotropy. After the film was cooled to the martensite state at 300 K, the shape of the magnetization loop changed significantly, and the coercivity increased drastically. In addition to a sharp increase at first (first quadrant in Fig. 1(b)), a step-increase occurs at 0.085 T. This typical magnetization behavior has been previously argued to originate from MIR.[9–11] The step-increase takes place between the fields of 0.085 T and 0.115 T, denoted as H_s and H_f, respectively, where the twin boundary motion occurs. As the field decreases from saturation field, the magnetization decreases by stages similar to the previous path, resulting in another hysteresis on the loop. This process indicates that the MIR is reversible.

The 7M martensitic phase, as in the present case, exhibits a (pseudo)-orthorhombic structure with one shortest axis, *c* axis, namely the easy magnetization axis. When the high temperature austenitic phase transforms into the martensitic phase, three different orientations of the martensitic *c* axis with respect to the cubic austenite cell are possible. However, without external stimuli, during martensitic transformation, the martensite *c* axis as well as the magnetic moment is preferably aligned within the film plane. Since the magnetic signal within the film plane could not be detected by magnetic tips, the as-deposited film showed featureless domain structure with weak contrast (Fig. 2(b)), which is similar to those shown in Refs. [14] and [15]. On the other hand, direct observation of the twin microstructure requires an epitaxial film with ultra-flat surface.[16,17] In polycrystalline Ni–Mn–Ga films with relatively rough surfaces, the twin microstructure is hardly revealed by surface probe means, such as AFM (Fig. 2(a)) or SEM.[18,19] As is well known, the martensitic variant with *c* axis inclined to an external magnetic-field is preferably nucleated when the austenitic phase transforms into martensitic phase with magnetic field cooling. Thus, a magnetic field perpendicular to the film plane is introduced to achieve the visible domain structure with distinct contrast by MFM. When the film was cooled down from 333 K to 300 K with a magnetic field of 0.02 T normal to the film plane, the magnetic moment of the film was partially aligned toward the external magnetic field, leading to the bright domain region shown in Fig. 2(c). As the cooling magnetic field is increased to 0.12 T, this large field is sufficiently high to orient all the magnetic moments in the film along the external field, as shown in Fig. 2(d). Magnetic domain structure is closely related to the microstructure,[20,21] allowing us to investigate the twinning structure of the Ni–Mn–Ga films by observing the evolution of the magnetic domain structure.

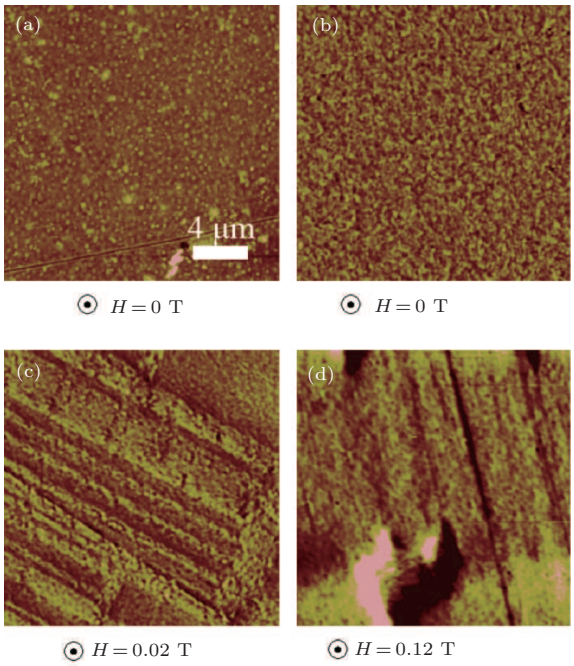


Fig. 2. (color online) Typical (a) AFM and (b) MFM images of surface morphology and domain structure, respectively, at 300 K for the as-deposited Ni–Mn–Ga film. Typical MFM images of domain structures at 300 K for the film cooling from 333 K to 300 K with magnetic fields of (c) 0.02 T and (d) 0.12 T normal to the film plane. All images were scanned in the range of 20×20 μm.

Figure 3 shows the evolution of domain structure in the temperature range of 318 K–300 K for the film with a magnetic field of 0.12 T, normal to the film plane. Before measurements, the film was heated to 333 K to obtain a fully austenitic structure. The magnetic domain structure presents a featureless MFM image (Fig. 3(a)) at 318 K, and rarely changes above 309 K, at which point the film is in the cubic austenitic phase. At 308 K, a few bright stripe-shaped domains emerge (Fig. 3(b)), consistent with starting temperature of the martensitic transformation. It is reasonable to deduce that the martensite variants with *c* axis inclined to the magnetic field are preferentially nucleated in the stripe domain. With decreasing temperature, the nucleation process continues (Fig. 3(c)), resulting in the increase of the number of stripe domains. When the temperature decreases to 305 K (Fig. 3(d)), some stripe domains start to grow and become wider. A further decrease of temperature leads to continuous growth of the width of the domains and the interconnection of some stripe domains (Fig. 3(e)). When the temperature decreases to 300 K, almost all stripe domains are interconnected and magnetic signals out of plane are detected (Fig. 3(f)). It is concluded that the martensitic transformation could be divided into two periods: nucleation and growth. One can note a difference between the thermomagnetic and MFM results — the martensitic transformation started at 309 K or 308 K according to the thermomagnetic and MFM measurements, respectively;

and it finished at 305 K or 303 K according to the thermomagnetic and MFM measurements, respectively. This discrepancy might be explained by the fact that the Ni–Mn–Ga film is grown on a substrate that was directly attached to the heating stage. Thus, there should be a temperature gradient between the film, which was exposed in the room temperature air, and the heating stage where the temperature was detected by the measurement system, resulting in the difference between the thermomagnetic and MFM results.

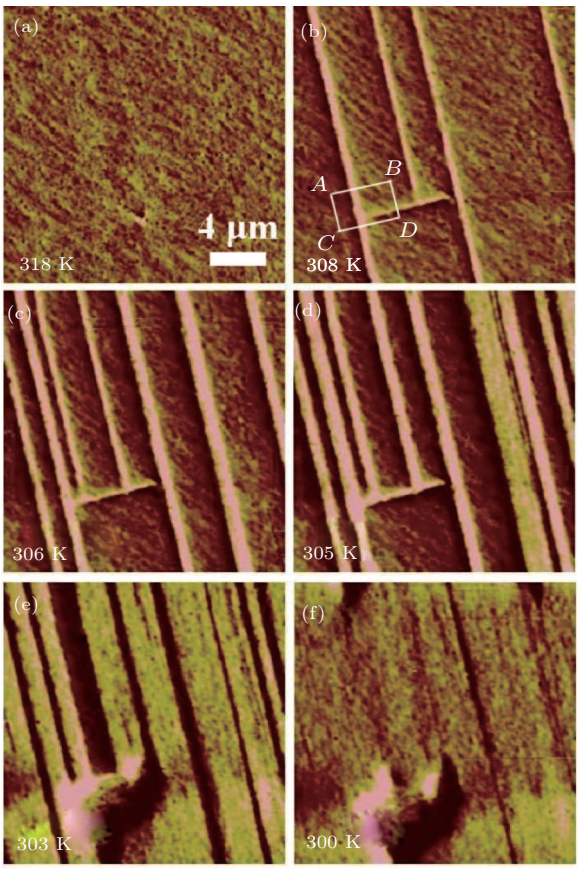


Fig. 3. (color online) *In situ* domain structure evolution for the Ni–Mn–Ga film, cooling to (a) 318 K, (b) 308 K, (c) 306 K, (d) 305 K, (e) 303 K, and (f) 300 K with a magnetic field of 0.12 T, normal to the film plane. All images were scanned in the range of 20×20 μm.

Attempts were made to understand the evolving microstructure of the film as it cooled under magnetic field, by a comparison of the crystallographic texture and the magnetic domain structure. When Ni–Mn–Ga films transform from austenite to martensite under magnetic field, martensitic variants with easy magnetization along the c axis, inclined to the direction of external field, are preferably nucleated. Considering the film contains {101}-oriented grains, and the martensitic phase has (pseudo)-orthorhombic structure, $a \neq b \neq c$, eight variants are adopted. Schematic representation of four variants, variants 1–4, is displayed in Fig. 4(a). Actually, the 7M martensitic phase has a slight monoclinic distortion to an orthorhombic unit cell,[5] which is ignored in this simplified model. The Miller indices are guides for eyes and discussion. The other four variants could be sketched by exchanging the a and b axes of variants 1–4, denoted as variants 1′–4′ by adding a superscript to corresponding variants 1–4. Here, only variant 1′ is presented; variants 2′–4′ can be obtained in the same manner. The c axis of variant 1–4 is neither perpendicular nor parallel to the film plane, but instead forms the angle θ, $\theta = \arctan(a/c)$; and likewise $\theta' = \arctan(b/c)$ for variants 1′–4′ is derived. In our experiment, the magnetic field is applied normal to the film plane during cooling, thus, the magnetostatic energies of the variants 1–4 and 1′–4′ under the external fields are given by

$$E = \mu_0 M_{\text{sat}} H \cos\theta \quad \text{and} \quad E' = \mu_0 M_{\text{sat}} H \cos\theta',$$

respectively, where μ_0 is the magnetic permeability of free space, H is magnetic field, M_{sat} is the saturation magnetization. Since $a > b$, then $\theta > \theta'$ and $E < E'$ are extracted. Therefore, variants 1–4 are energetically favored to nucleate under magnetic field normal to the film plane, compared with variants 1′–4′. It is worth noting that variants 1–2 and variants 3–4 can be classified as two sets of perpendicular-oriented grains, which are inherited from the austenitic phase rather than formed through the martensitic transformation; in other words, variants 1–2 do not share a twinning relationship with variants 3–4, which was previously reported in Ref. [11].

Figure 4(b) shows a schematic diagram of microstructure and its corresponding domain structure to produce the MFM image of the *ABCD* zone in Fig. 3(b). As we know, polycrystalline Ni_2MnGa austenite has a cubic unit cell with lattice constant a_A=0.5821 nm. A misfit of the lattice is calculated as low as 0.06% between the direction of $[101]_M$ and $[101]_A$ and 0.19% between the $[010]_M$ and $[010]_A$, suggesting that the $(101)_M$ plane is energetically favored to be the interface between austenite and martensite.[22] Based on this understanding, a phenomenological model is proposed to determine the microstructure of the stripe domains. Since one of the two $[101]_M$ faces of variants 1–4 is parallel to the film plane, the other one should be the austenite–martensite interface (reads as *A*–*M* interface in Fig. 4(b)) along the sides of the stripe domain, indicating that the b axis of the martensitic unit cell is aligned along the length of the stripe domains. For the stripe domain 1, variants 1 and 2 with b axis along the length of the stripe are selectable. However, stripe domain 1 in single-variant state of variant 1 or 2 results in equivalent shear strain with opposite sign, compared with that in austenitic state. To accommodate stress resulting from martensitic transformation, stripe domain 1 should be in a twinned microstructure of variants 1 and 2. An individual cell of variant 1 near the surface is depicted in Fig. 4(b); its crystallographic axes, a, b, and c, are marked with bold lines. It is also depicted that the normal component of the magnetization of twin variant results in the stripe domain. In the same manner, the microstructure of stripe domain 2 is determined to be the twinning of variants 3 and 4.

As mentioned above, variants 1–2 do not share a twinning relationship with variants 3–4; stripe domain 2 still exists when the martensitic transformation finishes (seen in Fig. 3(f)). The present results reflect that the microstructure gives rise to a unique magnetic domain pattern, which in turn, is manifest in a distinctive MIR response, as discussed below.

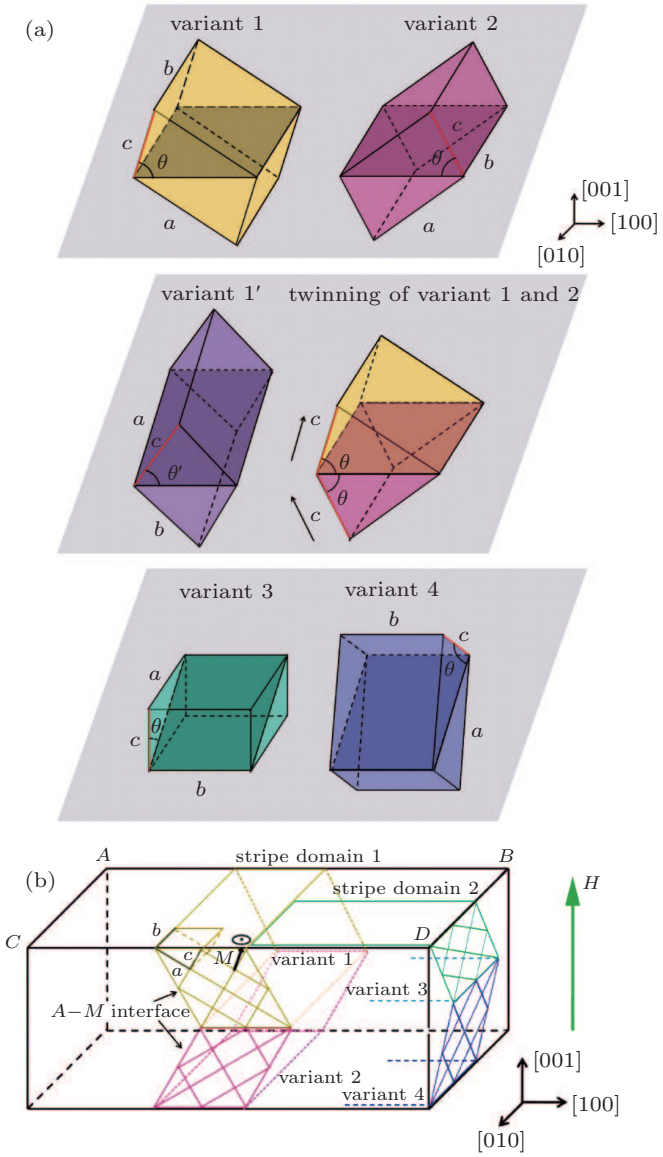


Fig. 4. (color online) (a) Schematic representation of the variants with the c axis inclined to the normal of the film plane. (b) Simplified schematic diagram of the twin and magnetic domain structure for *ABCD* zone in Fig. 3(b). The Miller indices are guides for the eyes.

Figure 5 shows the evolution of domain structure with the magnetic field, parallel to the film plane, increasing from 0 T to 0.15 T then back to 0 T. The film was pre-treated by cooling to 308 K under an out-of-plane magnetic field of 0.12 T then cooling to room temperature (RT) without magnetic field. Here, the film is intentionally cooled to 308 K, the beginning of martensitic transformation in which the film has a stripe domain structure (as shown in Fig. 3(b)) and a defined twinning structure, as discussed above. After cooling to RT without magnetic field, the bright stripe domains are divided into domain chains, where bright and dark sub-domains are arranged alternately, to minimize the demagnetization energy. Microstructure in the stripe domain region is retained by the pre-treatment. In other words, the c axis of the variants, both in the chaining domain region and in the stripe domain region, is inclined to the normal of the film plane. One typical chaining domain is marked by the white dashed line in Fig. 5(a). When the magnetic field increased to 0.075 T, the trace of chaining domains could still be observed but its contrast became weak (shown in Fig. 5(b)). With the magnetic field increased to 0.15 T, the chaining domains disappeared (Fig. 5(c)). One can see magnetic domains with weak contrast spreading along the direction of the magnetic field; magnetic moments in the film are aligned along/inclined to the magnetic field direction. The weak magnetic contrast is ascribed to the out-of-plane component of the magnetic moments, switching between being "in" and "out" of the surface of the film. Subsequently, the magnetic field was decreased to 0 T, and no chaining domains or stripe domains were observed to be reversible (Fig. 5(d)); meanwhile, no well-defined magnetic domain can be seen, indicating the martensite c axis in the entire film is aligned within/inclined to the film plane. Considering that the M–H curve predicts significant remanence in the martensitic state (Fig. 1(b)), magnetic moments are thought to be inclined to the film plane but distributed randomly.

The evolution of magnetic domain structure is attributed to the reorientation of the twin variants of martensite. A simplified three-dimensional (3D) schematic diagram of the twin and magnetic domain structure is shown in Fig. 5(e) to clarify the mechanism. This chaining domain has been observed in bulk Ni–Mn–Ga, and is due to the normal component of magnetization pointing up or down.[23] In our case, to avoid generating poles at the twin boundary, the two twin-related variants in the chaining domain region should have their magnetization directions pointing both up or both down (refer to the twinning relationship of variants 1 and 2 in Fig. 4(a)), giving rise to the overall magnetization (arrows in dashed line) of the twinned structure pointing toward the film surface or away from it. While it is somewhat complicated to ascertain the microstructure of the later-transformed region, the region transforms to martensite after removing the magnetic field normal to the film plane, between the chaining domains, as $(202)_M$, $(220)_M$, and $(022)_M$ peaks are observed in the XRD spectrum (which is obtained with no applied field). In this model, we adopt the variant with c axis parallel to the film plane. Adjacent variants with different orientations could be connected by twin boundaries;[24] although the variants in the chaining domain share ac twin boundary, the twinning variants of the orthorhombic structure provide additional twinning degrees of freedom to connect the two regions. This microstructure al-

lows the occurrence of complex MIR by expanding the proportion of martensitic variants at the expense of the variants with higher magnetostatic energy, through twin-boundary motion driven by magnetic field.[25] One can imagine that when the in-plane field increases, magnetic moments in the chaining domain region first rotate to the field direction, resulting in the weak contrast of chaining domains (Fig. 5(b)). When the magnetic field increases to the critical value to trigger the twin-boundary motion, the MIR takes place and the variants in the later-transformed region expand at the expense of the variants in the chaining domain, the magnetization in the chaining domain region changes from perpendicular to parallel to the film plane, giving rise to the irreversible vanishing of chaining domains.

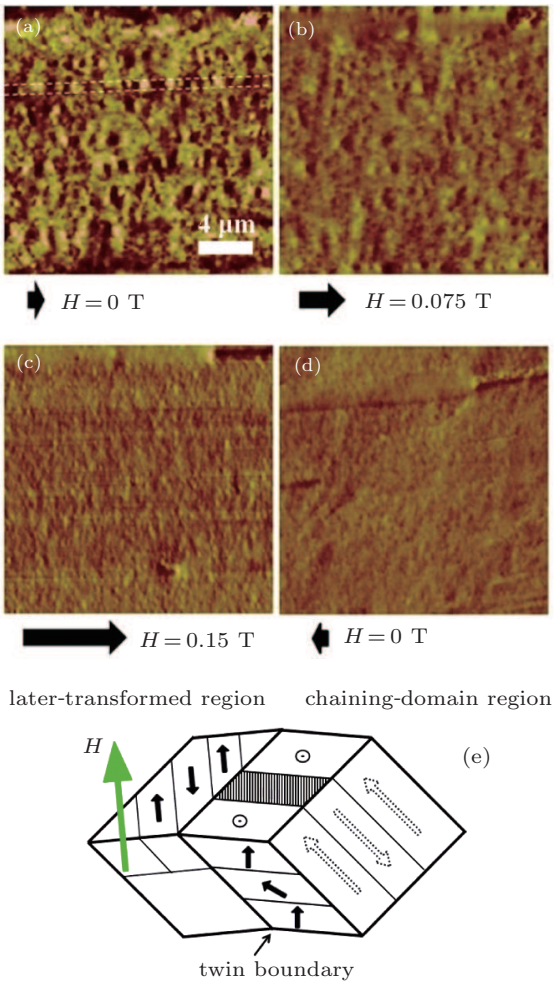


Fig. 5. (color online) *In situ* domain structure, obtained with an applied magnetic field parallel to the film plane, increasing from (a) 0 T via (b) 0.075 T to (c) 0.15 T then decreasing to (d) 0 T. All images were scanned in the range of 20×20 μm. (One of the chaining domains is outlined by a white dashed line). (e) Simplified 3D schematic diagram of the twin and magnetic domain structure.

4. Conclusion

In summary, Ni–Mn–Ga film with 7M modulated martensitic structure was prepared on MgO (001) substrate. A typical hysteresis on the magnetization curve indicates the existence of MIR. Based on the correlation of magnetic domain structure and microstructure, the martensitic transformation and reorientation process were observed by the evolution of the magnetic domain structure. It is found that martensitic transformation could be divided into two parts: nucleation and growth. The twin variants can be identified by a comparison of the crystallographic texture and the magnetic domain structure. For the thermo-magnetically treated film, cooling with magnetic field to a stripe domain state, then cooling without magnetic field to RT, the stripe domains change into chaining domains due to the demagnetizing field. When the magnetic field was applied parallel to the pre-treated film plane, the chaining domains irreversibly vanished, which is attributed to the reorientation of martensite. The present method of thermo-magnetic treatment could be developed into an alternative and convenient route to investigate the microstructure of FSM alloys.

References

[1] Ullakko K, Huang J K, Kantner C and O'Handley R C 1996 *Appl. Phys. Lett.* **69** 1966
[2] Murray S J, Marioni M, Allen S M, O'Handley R C and Lograsso T A 2000 *Appl. Phys. Lett.* **77** 886
[3] Sozinov A, Lanska N, Soroka A and Zou W 2013 *Appl. Phys. Lett.* **102** 021902
[4] Sozinov A, Likhachev A A and Ullakko K 2002 *IEEE Trans. Magn.* **38** 2814
[5] Pons J, Chernenko V A, Santamarta R and Cesari E 2000 *Acta Mater.* **48** 3027
[6] Liu Z H and Ma X Q 2012 *Acta Phys. Sin.* **61** 028103 (in Chinese)
[7] David D C and Müllner P 2011 *Adv. Mater.* **23** 216
[8] Zeng M, Or S W, Zhu Z Y and Ho S L 2010 *J. Appl. Phys.* **108** 051716
[9] Heczko O, Thomas M, Buschbeck J, Schultz L and Fähler S 2008 *Appl. Phys. Lett.* **92** 072502
[10] Thomas M, Heczko O, Buschbeck J, Rößler U K, McCord J, Scheerbaum N, Schultz L and Fähler S 2008 *New J. Phys.* **10** 023040
[11] Zhang Y P, Hughes R A, Britten J F, Preston J S, Botton G A and Niewczas M 2010 *Phys. Rev. B* **81** 054406
[12] Yeduru S R, Backen A, Kübel C, Wang D, Scherer T, Fähler S, Schultz L and Kohl M 2012 *Scr. Mater.* **66** 566
[13] Heczko O, Straka L, Lanska N, Ullakko K and Enkovaara J 2002 *J. Appl. Phys.* **91** 8228
[14] Chernenko V A, Anton R L, Kohl M, Ohtsuka M, Orue I and Barandiaran J M 2005 *J. Phys: Condens. Matter* **17** 5215
[15] Chernenko V A, Anton R L, Barandiaran J M, Orue I, Besseghini S, Ohtsuka M and Gambardella A 2008 *IEEE Trans. Magn.* **44** 3040
[16] Buschbeck J, Niemann R, Heczko O, Thomas M, Schultz L and Fähler S 2009 *Acta Mater.* **57** 2516
[17] Eichhorn T, Hausmanns R and Jakob G 2011 *Acta Mater.* **59** 5067
[18] Tillier J, Bourgault D, Barbara B, Pairis S, Porcar L, Chometon P, Dufeu D, Caillault N and Carbone L 2010 *J. Alloys Compd.* **489** 509
[19] Wang H B, Liu C, Lei Y C and Cai W 2008 *J. Alloys Compd.* **465** 458
[20] Lai Y W, Schäfer R, Schultz L and McCord J 2010 *Appl. Phys. Lett.* **96** 022507
[21] Reinhold M, Watson C, Knowlton W B and Müllner P 2010 *J. Appl. Phys.* **107** 113501
[22] Bhattacharya K, Purohit P and Craciun B 2003 *J. Phys. IV France* **112** 163
[23] Pan Q and James R D 2000 *J. Appl. Phys.* **87** 4702
[24] Liu C, Mu H W, Gao L X, Ma W J, An X, Gao Z Y and Cai W 2010 *Appl. Surf. Sci.* **256** 6655
[25] Wang J M, Wang Y F, Jiang C B and Xu H B 2006 *Chin. Phys. Lett.* **23** 1293